Radar Target Simulation Based on Measurement Data

Pirmin Schoeder, Timo Grebner, Vinzenz Janoudi, Christian Waldschmidt
Institute of Microwave Engineering, Ulm University, Ulm, 89077 Germany
{name.surname}@uni-ulm.de

***Abstract*— The repeatability of radar sensor tests is of high importance, in order to allow for a better comparability. Guaranteeing consistent test conditions is therefore essential. This article describes a radar target simulator able to simulate a traffic scenario for chirp-sequence frequency modulated continuous wave radar sensors, based on measurement data. First, the system setup is briefly presented, that is used to generate the targets, afterwards the major challenges and required signal processing steps are laid out. Finally, a comparison between the original measured scenario data and the replayed version is conducted.**

***Keywords*— automotive, radar, radar target simulator, signal processing, simulation.**

I. Introduction

The continuous advances in automotive sensor technology allow for more accurate and highly resolved measurements of a vehicle's environment. Radar sensors offer robustness due to their low dependence on weather conditions [1], [2]. Therefore, radar plays an important role to achieve the goal of increasing the reliable automatization of driving. In order to test advanced driver assistance systems (ADAS), test rides are indispensable. Since these rides cannot be repeated precisely, the direct comparison between sensors or the iterations of a sensor within the same scenario is almost impossible. To solve the issue of repeatability, a radar target simulator (RTS) could be employed to simulate an identical test ride multiple times. RTSs offer the possibility to simulate radar targets repeatedly under consistent conditions. Due to the required complexity of the simulated scenario, which includes multiple targets at individual ranges, velocities, and DOAs, a modulation-based RTS with flexible DoA simulation capabilities is used [3]. Modulation-based RTSs can simulate a high number of targets at close ranges for chirp-sequence frequency modulated continous wave (CS-FMCW) radars. Therefore, the most important properties of targets in automotive scenarios can be simulated. The system demonstrated in this article is able to replay a performed radar measurement for a radar sensor under test (RuT) in a controlled environment without the requirement of synchronization between RuT and RTS. Further, the frame rate and ramp parameters of the radar utilized for recording and the RuT can be chosen arbitrarily. The required signal processing chain applied to convert the raw measurement data into the modulation signal of the RTS is presented.

II. System Overview

For the system concept, an RTS is used in conjunction with a CS-FMCW radar sensor. The RTS is able to simulate multiple targets with individual range, velocity, direction-of-arrival (DoA), and radar cross section (RCS). The RuT and RTS are not synchronized, thus, this allows the use of two fully separated systems. The only requirement on the radar is the accessibility of the raw samples in order to calibrate the DoA simulation. The ramp parameters of the radar are assumed to be known. In c0ase this assumption is invalid, the system could be extended with an estimator [4]. The system's input is recorded radar data divided into frames, which is then processed to identify the significant targets for each frame, and those are then simulated for the RuT. The frame rate of the recorded measurements to be simulated is adopted by the RTS. In order to replicate a given scenario, the required modulation signal employed by the target simulator is the sum of complex sinusoids, each representing a single target. For the simulation of a single target, the radar signal is modulated with a sinusoid $x(t)$. The Amplitude A of the sinusoid determines the simulated target RCS, the frequency f_{mod}, the target's range R and the Doppler frequency shift f_{D}. The modulation frequency is calculated as [5]

$$f_{\mathrm{mod}} = \frac{1}{T_{\mathrm{C}}} \left\lfloor \frac{2R \cdot S \cdot T_{\mathrm{C}}}{c_0} \right\rceil + f_{\mathrm{D}}\,, \tag{1}$$

where $\lfloor \cdot \rceil$ denotes rounding to the nearest integer, S is the slope of the chirp, and T_{C} is the ramp repetition period. The RTS consists of four target elements (TE). The combination of multiple TEs allows to simulate the targets' DoA [3]. The

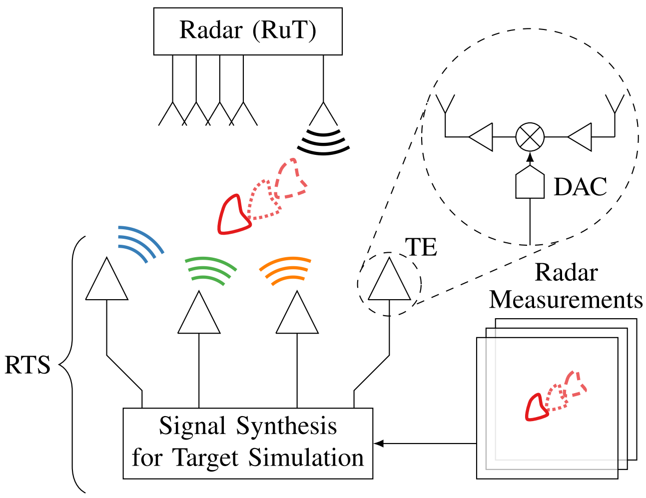

Fig. 1. System setup used to simulate recorded radar data.

ISBN 978-3-9820397-2-5 © IMA e.V. • Ratingen, Germany

Authorized licensed use limited to: KIZ Abt Literaturverwaltung. Downloaded on July 04,2022 at 10:27:05 UTC from IEEE Xplore. Restrictions apply.

TEs are modulating the radar transmit signal with the same frequencies for each (k-th) target, but the sinusoids' amplitudes $A_{k,m}$ and phases $\phi_{k,m}$ depend on the TE's position and the simulated DoA. The modulation signal $s_{\mathrm{mod},m}(t)$ of the m-th TE is therefore

$$\begin{aligned} s_{\mathrm{mod},m}(t) &= \sum_{k=1}^{K} x_k(t) \\ &= \sum_{k=1}^{K} A_{k,m} \exp(\mathrm{j}2\pi f_{\mathrm{mod},k} t + \mathrm{j}\phi_{k,m}) \,. \end{aligned} \tag{2}$$

At the radar receive antennas, the superposition of the modulated chirps, originating from different TEs, determines the simulated DoA.

III. Signal Processing

The general steps for simulating measured data with the system is described within this section. The signal processing chain converts the raw data of the recording radar system into the modulation signal required to simulate the measured data.

A. Relevant Target Extraction

While the amount of targets that can be simulated simultaneously is theoretically unlimited, the combined simulated backscattered power is limited by the maximum modulation amplitude provided by the DAC. Therefore, the available power should be only utilized to simulate significant targets. Every Rv-cell of the recorded data could be translated into a target with range, velocity, DoA, and RCS. But modulating an Rv-cell that only contains noise would lower the available power for relevant targets. Therefore, the original recorded data has to be reduced to relevant targets. The reduced target list can be created and the modulation signal calculated via (2). Therefore, the first steps for the signal processing chain are similar to traditional CS-FMCW signal processing. The Rv-matrix is generated by windowing and applying a 2D-fast Fourier transform (FFT). Afterwards, a constant false alarm rate (CFAR) algorithm is employed to select only the relevant cells. Cells that are close to the sensor without a velocity are discarded, since the simulation of the radar leakage signal is not desired, as it is an effect of the radar itself and not of the environment. For each remaining Rv-cell, a DoA estimation is performed, the modulation frequency $f_{\mathrm{mod},k}$ is calculated, and the required amplitudes $A_{k,m}$ and phases $\phi_{k,m}$ for the TEs are determined.

B. Modulation Signal Synthesis

The next step is to generate the modulation signal for each frame by calculating the sum of sinusoids using (2). As the number of targets increases, the direct synthesis increases in computational complexity. Therefore, the faster implementation using an inverse FFT (IFFT) is chosen [6]. The computational complexity of the modulation signal systhesis does therefore not scale with the amount of targets, since the complexity of the IFFT only depends on the number of samples N within an RTS frame. The values of the frequency

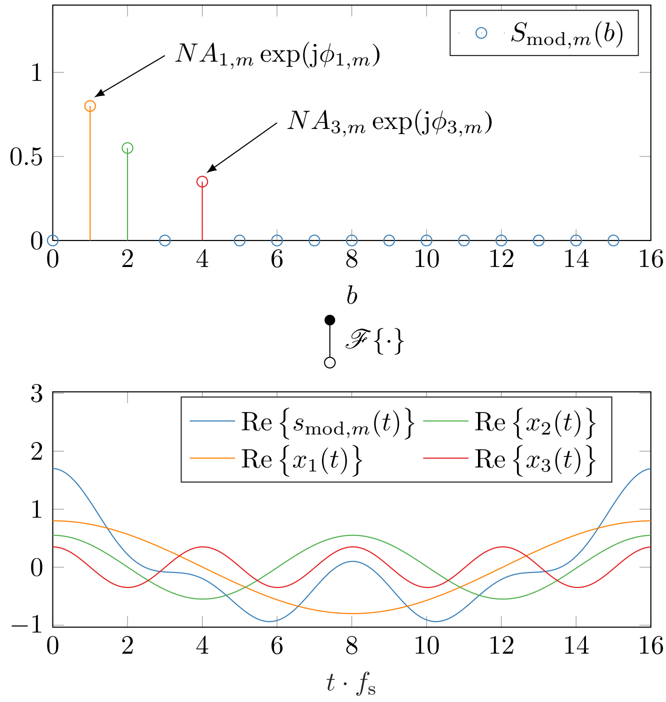

Fig. 2. Synthesis of the modulation signal $s_{\mathrm{mod},m}(t)$ in the frequency domain.

representation $S_{\mathrm{mod},m}(b)$ (b=0, 1, ...N−1) are set to the values of the desired amplitudes and phases at the frequency bins b_k:

$$S_{\mathrm{mod},m}(b) = \begin{cases} NA_{k,m}\exp(\mathrm{j}\phi_{k,m})\,, & b = b_k \\ 0\,, & \text{else} \end{cases} \,. \tag{3}$$

The frequency bins b_k are the ones closest to the desired modulation frequency $f_{\mathrm{mod},k}$, normalized by the DACs sampling rate f_s. Hence, the bins b_k represent discrete frequencies of

$$\tilde{f}_{\mathrm{mod},k} = b_k \frac{f_\mathrm{s}}{N} = \left\lfloor \frac{f_{\mathrm{mod},k}}{f_\mathrm{s}} N \right\rceil \frac{f_\mathrm{s}}{N} \,. \tag{4}$$

Calculating the IFFT of $S_{\mathrm{mod},m}(b)$ results therefore in the time-discrete values of the modulation signal

$$\begin{aligned} s_{\mathrm{mod},m}(n) &= \frac{1}{N}\sum_{b=0}^{N-1} S_{\mathrm{mod},m}(b)\exp\left(\mathrm{j}2\pi\frac{b}{N}n\right) \\ &= \frac{N}{N}\sum_{b_k} A_{k,m}\exp\left(\mathrm{j}2\pi\frac{\tilde{f}_{\mathrm{mod},k}}{f_\mathrm{s}}n + \mathrm{j}\phi_{k,m}\right) \,. \end{aligned} \tag{5}$$

For each TE this procedure is repeated as required by the DoA concept.

C. Frame Transition

For each frame the sum of sinusoids is now at hand. But since the radar simulator and the radar under test are not synchronized, the radar simulator might start a new frame, while the radar is still recording a frame. This causes a

ISBN 978-3-9820397-2-5 © IMA e.V. • Ratingen, Germany

Authorized licensed use limited to: KIZ Abt Literaturverwaltung. Downloaded on July 04,2022 at 10:27:05 UTC from IEEE Xplore. Restrictions apply.

discontinuity in the time domain and additional undesired spectral components in the frequency domain of the RuT baseband. In order to reduce the leakage caused by the discontinuity, the modulation signal is multiplied with a frame synthesis window function $w(n)$, overlapped and added with its neighboring frames. The degree of overlap is determined by the applied synthesis window function in order to maintain a constant overlap-add (COLA) property [7]

$$\sum_{l=-\infty}^{\infty} w(n + l \cdot N) = 1 \,. \tag{6}$$

A compromise between leakage in the frequency domain and temporal resolution of the targets has to be found. We choose a Tukey-window

$$w(n) = \begin{cases} \frac{1}{2} + \frac{1}{2}\cos\left(\frac{2\pi}{\alpha}\left(\frac{n}{N-1} - \frac{\alpha}{2}\right)\right), & \frac{n}{N-1} < \frac{\alpha}{2} \\ 1\,, & \frac{\alpha}{2} \leq \frac{n}{N-1} < 1 - \frac{\alpha}{2} \\ \frac{1}{2} + \frac{1}{2}\cos\left(\frac{2\pi}{\alpha}\left(\frac{n}{N-1} + \frac{\alpha}{2}\right)\right), & 1 - \frac{\alpha}{2} \leq \frac{n}{N-1} \end{cases} \tag{7}$$

with N the number of total samples in an RTS frame and the roll-off factor α. A rolloff factor of α=0.5 is chosen in order to achieve a 50 % overlap and thus maintain a high resolution in the time domain.

A simulated comparison for the worst case scenario of the resulting Rv-plot is depicted in Fig. 3. It is assumed that the RuT is windowing the data before applying the 2D-FFT that has lower spectral leakage than the Tukey-window like a Hann or Blackman-Harris-window [8]. Without the application of the Tukey-window, the frequency response of the discontinuity is visible by the high spectral components in the velocity dimension. Due to the overlap of the RTS frames, the number of samples in each frame is increased by the overlap factor. In the case of a Tukey-window with rolloff α the number of samples N in each frame is $1+\alpha$ times higher than in the hard transition case. Since each frame consists of stationary sinusoids, additional samples of the modulation signal can be calculated before the application of the window by scaling the value of samples per frame N proportionally.

IV. Measurements

In this section, performed measurements are presented to confirm the functionality of the system and the proposed signal processing.

A. Frame Transition

In order to show the effect of the frame transition using a Tukey-window with the proposed overlap add scheme, a scenario with a point target is simulated. The target switches its speed each frame between $7\,\mathrm{m\,s^{-1}}$ and $-7\,\mathrm{m\,s^{-1}}$. If the RTS changes its frame during the RuT frame, both targets are visible in the Rv-plot, and the effect of the frame transition is visible. In Fig. 4, the resulting Rv-plots simulating the scenario with the hard frame transition and the proposed COLA transition using a Tukey-window are shown. In case

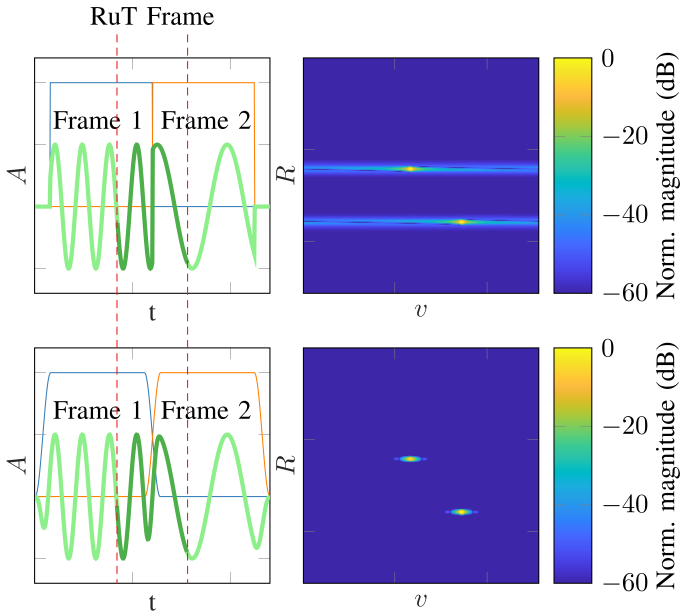

Fig. 3. Resulting Rv-plots (right) of frame transitions with no windowing and overlap (top) compared to Tukey-windowing, overlap and add (bottom).

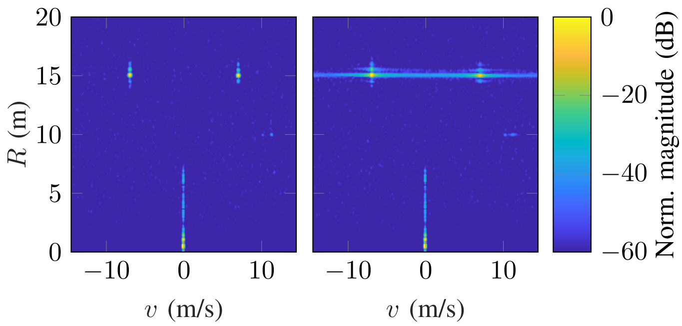

Fig. 4. Measured frame transition with a Tukey-window overlap add (left) and with a hard frame transition (right).

of the hard transition, the high leakage is visible, while the COLA transition is able to reduce the leakage due to the lower side-lobes of the Tukey-window in the frequency domain.

B. Simulation of Measurement Data

For the simulation of measured data, two kinds of measurements were performed. First, a parking lot scenario was recorded with a radar sensor attached to a car. The data resulting from this measurement is applied as input

Fig. 5. Measurement setups used to record (left) and to simulate (right).

ISBN 978-3-9820397-2-5

© IMA e.V. • Ratingen, Germany
Authorized licensed use limited to: KIZ Abt Literaturverwaltung. Downloaded on July 04,2022 at 10:27:05 UTC from IEEE Xplore. Restrictions apply.

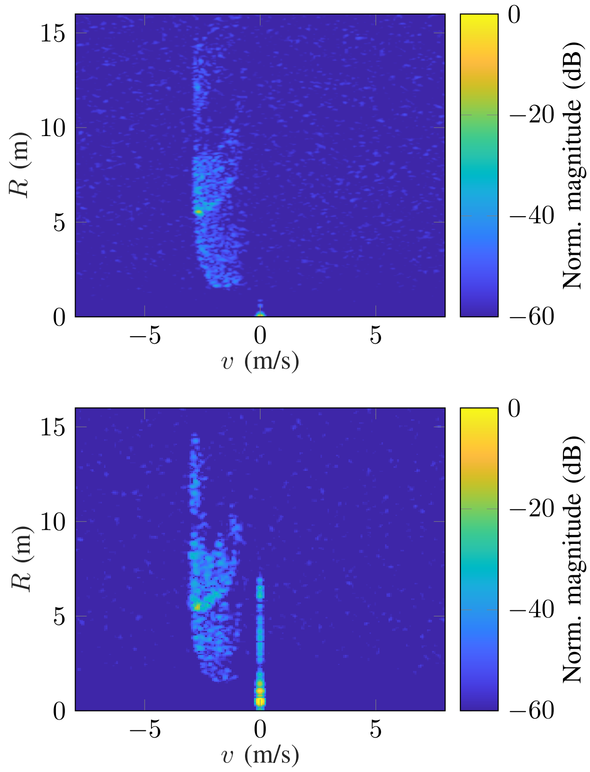

Fig. 6. Rv-plot comparison of original data (top) and simulated data (bottom).

for the signal processing chain in order to calculate the required modulation signal. This allows the simulation of the same parking lot scenario with the RTS. The recording radar sensor captures frames with a rate of 37 Hz and a bandwidth of 3 GHz. The target simulation was conducted in an anechoic chamber with the RTS, simulating the scenario to an RuT with 2 GHz bandwidth and a frame rate of 25 Hz. The data of the original measurement is then compared with the data resulting from the simulated version. In Fig. 5, the measurement setups for recording the original data and simulating the measurement are depicted. A qualitative comparison between the original measurement and the simulated version in Fig. 6 shows that the simulation was successful. Even though different ramp parameters were used when the original measurement data was recorded, the simulated version contains the relevant information velocity, range, and amplitude. The main difference are the static targets due to the target simulator itself and the anechoic chamber in the simulated measurement. The CFAR applied to extract the important Rv-cells of the recorded measurements was set to include most of the clutter but reject Rv-cells containing noise. In Fig. 7, the $R\theta$-plot the successful simulation of the DoA property of targets is visible as well. The maximum magnitude for all velocities with $v{\neq}0\,\mathrm{m\,s^{-1}}$ is displayed.

V. Conclusion

In this work a system is presented that enables the simulation of measured radar data in a controlled environment

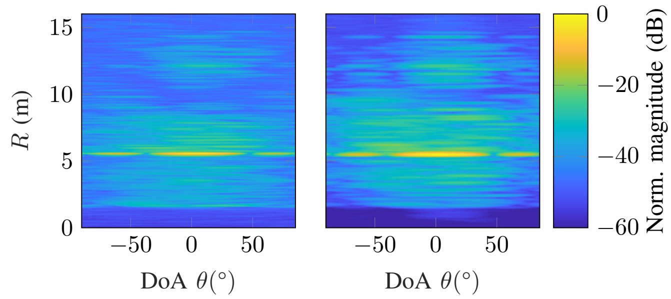

Fig. 7. Comparison of DoA between original data (left) and simulated data (right).

for another radar with different parameters. Complex scenarios containing multiple targets with all relevant target parameters (range, Doppler-shift, RCS, and DoA), extracted from measured data, can be simulated. A signal processing chain is proposed, allowing to overcome the main challenges that arise with unsynchronized systems and high radar target counts. Measurements confirm the functionality of the system and signal processing chain.

Acknowledgment

This work was supported by the German Federal Ministry of Education and Research (BMBF) and the Federal States of Germany under grant “Innovative Hochschule” (FKZ) 03IHS024D. The responsibility for the content of this publication lies with the authors.

References

[1] J. Hasch, E. Topak, R. Schnabel, T. Zwick, R. Weigel, and C. Waldschmidt, “Millimeter-wave technology for automotive radar sensors in the 77 GHz frequency band,” *IEEE Trans. on Microw. Theory and Techn.*, vol. 60, no. 3, pp. 845–860, 2012.

[2] C. Waldschmidt, J. Hasch, and W. Menzel, “Automotive radar — from first efforts to future systems,” *IEEE J. Microwaves*, vol. 1, no. 1, pp. 135–148, Jan. 2021.

[3] P. Schoeder, V. Janoudi, B. Meinecke, D. Werbunat, and C. Waldschmidt, “Flexible direction-of-arrival simulation for automotive radar target simulators,” *IEEE J. Microwaves*, vol. 1, no. 4, pp. 930–940, Oct. 2021.

[4] P. Schoeder, B. Schweizer, A. Grathwohl, and C. Waldschmidt, “Multitarget simulator for automotive radar sensors with unknown chirp-sequence modulation,” *IEEE Microw. Wireless Compon. Lett.*, vol. 31, no. 9, pp. 1086–1089, 2021.

[5] J. Iberle, P. Rippl, and T. Walter, “A near-range radar target simulator for automotive radar generating targets of vulnerable road users,” *IEEE Microw. and Wireless Compon. Lett.*, vol. 30, no. 12, pp. 1213–1216, 2020.

[6] H. Chamberlin, *Musical Applications of Microprocessors*. USA: Hayden Books, 1987.

[7] R. Crochiere, “A weighted overlap-add method of short-time Fourier analysis/synthesis,” *IEEE Trans. on Acoust., Speech, Signal Process.*, vol. 28, no. 1, pp. 99–102, 1980.

[8] F. Harris, “On the use of windows for harmonic analysis with the discrete Fourier transform,” *Proceedings of the IEEE*, vol. 66, pp. 51 – 83, 02 1978.

ISBN 978-3-9820397-2-5

© IMA e.V. • Ratingen, Germany

Authorized licensed use limited to: KIZ Abt Literaturverwaltung. Downloaded on July 04,2022 at 10:27:05 UTC from IEEE Xplore. Restrictions apply.